Organic Geochemistry 47 (2012) 1–8

Contents lists available at SciVerse ScienceDirect

Organic Geochemistry

journal homepage: www.elsevier.com/locate/orggeochem

Variation in abundance and distribution of diamondoids during oil cracking

Chenchen Fang, Yongqiang Xiong *, Qianyong Liang, Yun Li

State Key Laboratory of Organic Geochemistry (SKLOG), Guangzhou Institute of Geochemistry, Chinese Academy of Sciences, Guangzhou 510640, PR China

ARTICLE INFO

Article history:
Received 14 October 2011
Received in revised form 20 December 2011
Accepted 2 March 2012
Available online 12 March 2012

ABSTRACT

In this study, changes in the abundance and distribution of diamondoids in petroleum with thermal maturity were investigated by a simulation oil cracking experiment. Highly sensitive and selective gas chromatography–triple quadrupole mass spectrometry (GC–MS–MS) was employed to quantify diamondoids at ppm and sub-ppm levels. The results indicate that diamondoids were generated primarily within the maturity range 1.0–2.1% EasyRo and destroyed at high thermal maturity (>2.1% EasyRo). Hence, the occurrence of high concentrations of diamondoids probably corresponds to the maturity range from the wet gas to the early dry gas stage (i.e., 1.5–2.5% EasyRo). Good correlations were observed between a few ratios of diamondoids (i.e., EAI, DMAI-1, DMDI-1 and TMAI-1) and EasyRo. This finding indicates that these parameters may be useful maturity indices for organic matter from the late oil window to the dry gas window.

1. Introduction

Diamondoids are cage hydrocarbons with diamond-like structures that have been detected in many crude oils (Wingert, 1992; Chen et al., 1996; Dahl et al., 1999), coals and sedimentary rocks (Schulz et al., 2001; Wei et al., 2006b). Their concentrations and distributions are considered to be dependent on thermal stress. Therefore, some diamondoid indices have been established to determine thermal maturity of source rocks and crude oils (Chen et al., 1996; Li et al., 2000; Zhang et al., 2005), and to assess the extent of oil cracking (Dahl et al., 1999). Calibrations between diamondoid parameters and maturity of source rocks are based on diamondoids in source rock extracts and thermal maturity indices of the corresponding rocks (Chen et al., 1996; Li et al., 2000). In this procedure, some interference from other factors, such as source rock organofacies is unavoidable. Hence, hydrous pyrolysis of immature source rocks and peats is another important approach to obtain calibrations between vitrinite reflectance and diamondoid concentrations (Wei et al., 2007a). The diamondoid–Ro relationship obtained from source rocks can then be used to evaluate the maturity of oils (Zhang et al., 2005).

The origin and formation mechanism of diamondoids in oils and source rock extracts remains unclear. Due to their absence in recent organic matter, diamondoids are not considered to have a biosynthetic origin, but are theorized to be generated during diagenesis and catagenesis of organic matter (Wei et al., 2006c, 2007a). The most frequently mentioned mechanism is the Lewis acid catalyzed rearrangement of potential precursors (Fort and Schleyer, 1964; Schneider et al., 1966; Petrov et al., 1974). Several organic components in sediments, kerogen and crude oils probably become precursors of diamondoids under thermal stress and in the presence of suitable catalysts (Wingert, 1992; Wei et al., 2006a,c; Giruts et al., 2006; Giruts and Gordadze, 2007; Gordadze and Giruts, 2008; Berwick et al., 2011). Diamondoids are produced during the pyrolysis of kerogen and modern sediments, and acidic clay minerals (e.g., aluminosilicates) promote the formation of diamondoids (Wei et al., 2006a,c). In addition, pyrolysis experiments also show that diamondoids can be derived from high molecular mass, saturated and polar fractions of crude oils (Giruts et al., 2006; Giruts and Gordadze, 2007). The characteristic abundance and distribution of diamondoids from the two different origins have not yet been quantitatively investigated.

Given their high structural stability, diamondoids are conserved and concentrated by long term geological processes. Dahl et al. (1999) suggested that once diamondoids form, they are neither destroyed nor created. As a result, the increase of diamondoid concentrations in petroleum was attributed to the thermal degradation of most other non-diamondoid compounds (Dahl et al., 1999). However, quantitative determination of diamondoids in the extracts of a suite of coals and rocks over a broad range of maturity (Ro = 0.20–6.40%) has shown that diamondoid destruction occurs at Ro > 4.0% (Wei et al., 2006b). Some diamondoid species may also be thermally degraded to aromatic hydrocarbons at high temperature (Oya et al., 1981; Schoell and Carlson, 1999; Wei et al., 2006b). For instance, a pyrolysis experiment on diamantane has proven that it is cracked to aromatic hydrocarbons, gases and pyrobitumen at high temperature (Wei et al., 2006b). Therefore, the evolution of diamondoids during thermal maturation needs to be better understood to construct diamondoid indices and predict their useful ranges.

* Corresponding author. Tel.: +86 20 85290744; fax: +86 20 85290706.
E-mail address: xiongyq@gig.ac.cn (Y. Xiong).

0146-6380/$ - see front matter © 2012 Elsevier Ltd. All rights reserved.
http://dx.doi.org/10.1016/j.orggeochem.2012.03.003

Because oils from the Tarim Basin in China are generally of very high thermal maturity, most biomarker maturity parameters are unavailable. The abundance and distribution of diamondoids have been measured in highly mature Tarim oils (Chen et al., 1996; Zhang et al., 2005; Li et al., 2010). However, the lack of effective calibrations between diamondoid parameters and maturity of oils limited the application of diamondoid indices. The purpose of this study is to characterize the changes in abundance and distribution of diamondoids during oil cracking, as well as to establish the correlation between diamondoid parameters and the extent of oil cracking by a simulation oil cracking experiment.

2. Materials and methods

2.1. Sample

A normal crude oil collected from the Tarim Basin in northwestern China was used in the present study. Quantitative analysis showed that this oil contained relatively low concentrations of adamantanes and diamantanes (10.1–46.9 ppm for individual compounds). To eliminate the effect of these diamondoids on the quantification of diamondoid generation during oil cracking, the oil sample was evaporated in a fume hood for 120 h prior to the pyrolysis experiment to remove the original adamantanes. The gas chromatogram showed that no C_6–C_{12} hydrocarbons remained in the evaporated oil and no adamantanes were detected by gas chromatography–triple quadrupole mass spectrometry (GC–MS–MS).

2.2. Simulation experiments

Simulation oil cracking experiments were carried out in sealed gold tubes (40 mm length, 5 mm i.d. and 0.5 mm wall thickness). The equipment and procedures for the pyrolysis experiments were described in a previous study (Xiong et al., 2004). Briefly, 20–50 mg oil samples were loaded into the gold tubes, which were subsequently flushed with argon for 5 min and sealed under an argon atmosphere. The tubes were placed in a series of stainless steel autoclaves. In each autoclave, three parallel gold tubes were placed to quantify gaseous hydrocarbons (C_1–C_5), gasoline hydrocarbons (C_6–C_{12}) and diamondoid hydrocarbons in pyrolysates. The autoclaves were heated in an oven at two constant heating rates of 20 °C/h and 2 °C/h. Twelve sampling points were set between 300 and 600 °C at intervals of ca. 24 °C. After heating, the autoclaves were removed from the oven and cooled in air. The pyrolysates were analyzed using GC and GC–MS–MS.

2.3. Determination of gaseous hydrocarbons

The first cleaned gold tube for each temperature point was placed in a vacuum glass system connected to GC inlet. After piercing the gold tube with a steel needle, gaseous hydrocarbons were released and introduced into the GC system. The individual gaseous hydrocarbons were quantified using an Agilent Technologies 6890 N gas chromatograph.

2.4. Determination of gasoline hydrocarbons

The parallel gold tube for gasoline hydrocarbon analysis was cooled for 25–30 min using liquid nitrogen and then rapidly cut in half and placed in a 4 ml sample vial filled with methanol. The gasoline hydrocarbons were ultrasonically extracted into the methanol. The composition of gasoline hydrocarbons in the pyrolysates was then analyzed using headspace single-drop

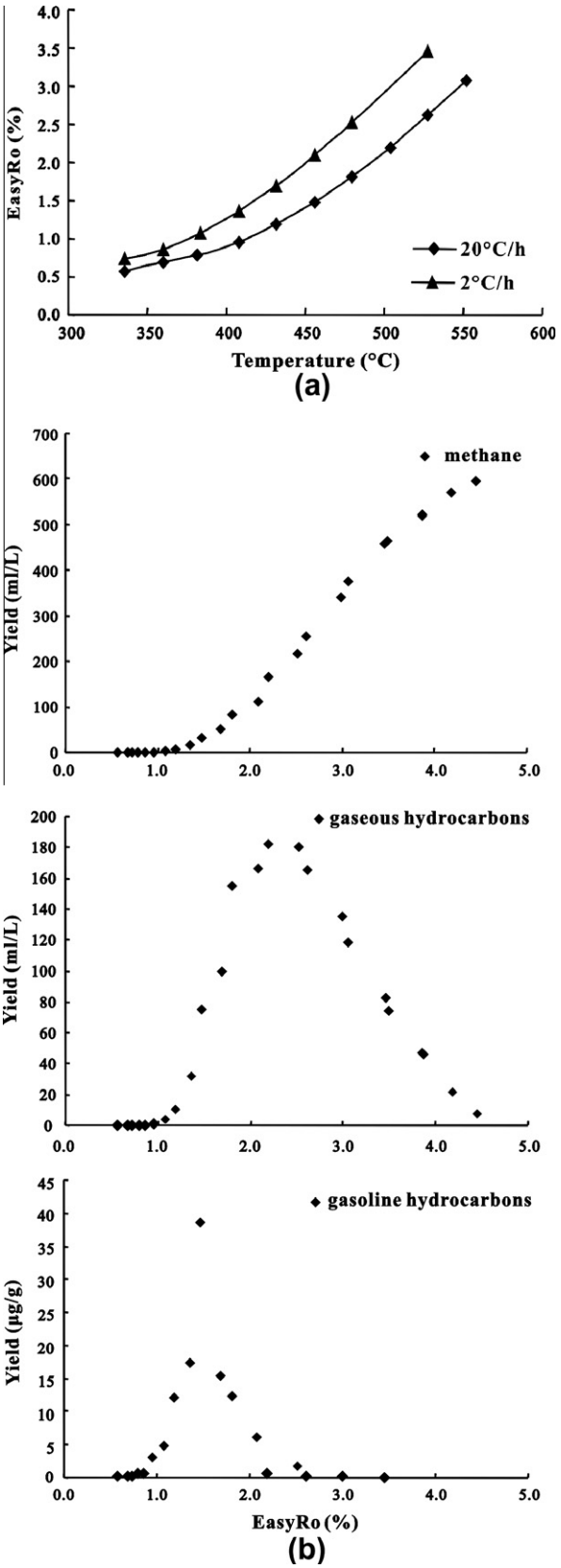

Fig. 1. Correlation among EasyRo (%), heating temperature (°C), and yields of hydrocarbons (ml/l or μg/g oil) in the laboratory oil-cracking experiments: (a) heating temperature versus EasyRo, (b) yields of different hydrocarbons (methane, C_2–C_5 gaseous hydrocarbons, C_6–C_{12} gasoline hydrocarbons) versus EasyRo. C_2–C_5 gaseous hydrocarbons include C_2, C_3, *i*-C_4, *n*-C_4, *i*-C_5, and *n*-C_5 alkanes, and C_6–C_{12} gasoline hydrocarbons refer to C_6–C_{12} *n*-alkanes.

microextraction coupled with GC-flame ionization detection (Fang et al., 2011).

2.5. Quantification of diamondoids

Similar to the determination of gasoline hydrocarbons, the other parallel gold tube for diamondoid analysis was first cooled for 25–30 min using liquid nitrogen, and then rapidly cut in half and placed in a 4 ml sample vial filled with isooctane. Next, about 50 µl isooctane with *n*-dodecane-d_{26} and *n*-hexadecane-d_{34} as internal standards were spiked into the sample vial. The vial was ultrasonically treated for 10 min to improve the dissolution of the analytes. After precipitating asphaltenes by centrifugation for 10 min, a volume of the supernatant was transferred into a 2 ml GC–MS–MS auto-sampler vial. The determination of diamondoids using the GC–MS–MS method was described in detail elsewhere (Liang et al., 2012).

3. Results and discussion

3.1. Extent of oil cracking

Petroleum is a complicated mixture and the proportion of its different components is variable during thermal maturation. Hence, the extent of oil cracking cannot be precisely determined using only the change in the petroleum bulk mass. In this study, the yields of methane, C_2–C_5 gaseous hydrocarbons and C_6–C_{12} gasoline hydrocarbons were used to evaluate the extent of oil cracking. The thermal maturation of oil in the simulation experiment was scaled with the vitrinite reflectance equivalence, which was calculated using the 'Easy%Ro' method of Sweeney and Burnham (1990). The purpose was to better extrapolate the results of the high temperature and fast simulation experiments to relatively low temperature and slow geological conditions. The model was considered to be applicable within the vitrinite reflectance range of 0.3–4.5% and within heating rates varying from 1 °C/week in the laboratory to 1 °C/10 my in geologic basins (Sweeney and Burnham, 1990).

The correlations among heating temperature, calculated Easy%Ro, and generation rates of different hydrocarbons (methane, C_2–C_5 gaseous hydrocarbons and C_6–C_{12} gasoline hydrocarbons) in the pyrolysates are displayed in Fig. 1. For each temperature point of the simulation experiment, the corresponding Easy%Ro and generation rates of different hydrocarbons were obtained and discussed below. Combined with the schematic diagram of generation and cracking of hydrocarbon products and pyrobitumen during oil cracking (Hill et al., 2003), the oil cracking process in this experiment can be classified into three main stages, namely, condensate, wet gas and dry gas. In the condensate stage (corresponding to 1.0–1.5% EasyRo), the generation rate of C_6–C_{12} hydrocarbons is greater than its decomposition rate. Accordingly, the yield of C_6–C_{12} hydrocarbons begins to increase at EasyRo of ca. 1.0%, and reaches the maximum at 1.5% EasyRo, indicating that oil cracking occurs at this stage. Subsequently, oil cracking enters the wet gas stage (corresponding to 1.5–2.1% EasyRo). In this stage, the yield of C_6–C_{12} hydrocarbons rapidly decreases, and that of C_2–C_5

Table 1
Peak identifications, formulas, and abbreviations of diamondoid compounds in the study.

Peak number	Molecular formula	Assignment	Abbreviation
1	$C_{10}H_{16}$	Adamantane	A
2	$C_{11}H_{18}$	1-Methyladamantane	1-MA
3	$C_{12}H_{20}$	1,3-Dimethyladamantane	1,3-DMA
4	$C_{13}H_{22}$	1,3,5-Trimethyladamantane	1,3,5-TMA
5	$C_{14}H_{24}$	1,3,5,7-Tetramethyladamantane	1,3,5,7-TeMA
6	$C_{11}H_{18}$	2-Methyladamantane	2-MA
7	$C_{12}H_{20}$	1,4-Dimethyladamantane(*cis*)	1,4-DMA(*cis*)
8	$C_{12}H_{20}$	1,4-Dimethyladamantane(*trans*)	1,4-DMA(*trans*)
9	$C_{13}H_{22}$	1,3,6-Trimethyladamantane	1,3,6-TMA
10	$C_{12}H_{20}$	1,2-Dimethyladamantane	1,2-DMA
11	$C_{13}H_{22}$	1,3,4-Trimethyladamantane(*cis*)	1,3,4-TMA(*cis*)
12	$C_{13}H_{22}$	1,3,4-Trimethyladamantane(*trans*)	1,3,4-TMA(*trans*)
13	$C_{14}H_{24}$	1,2,5,7-Tetramethyladamantane	1,2,5,7-TeMA
14	$C_{12}H_{20}$	1-Ethyladamantane	1-EA
15	$C_{12}H_{20}$	2,6- + 2,4-Dimethyladamantane	2,6- + 2,4-DMA
16	$C_{13}H_{22}$	1-Ethyl-3-methyladamantane	1-E-3-MA
17	$C_{13}H_{22}$	1,2,3-Trimethyladamantane	1,2,3-TMA
18	$C_{14}H_{24}$	1-Ethyl-3,5-dimethyladamantane	1-E-3,5-DMA
19	$C_{12}H_{20}$	2-Ethyladamantane	2-EA
20	$C_{14}H_{24}$	1,3,5,6-Tetramethyladamantane	1,3,5,6-TeMA
21	$C_{14}H_{24}$	1,2,3,5-Tetramethyladamantane	1,2,3,5-TeMA
22	$C_{15}H_{26}$	1-Ethyl-3,5,7-trimethyladamantane	1-E-3,5,7-TMA
I.S.-1	$C_{12}D_{26}$	*n*-Dodecane-d_{26}	*n*-C_{12}-d_{26}
23	$C_{14}H_{20}$	Diamantane	D
24	$C_{15}H_{22}$	4-Methyldiamantane	4-MD
25	$C_{16}H_{24}$	4,9-Dimethyldiamantane	4,9-DMD
26	$C_{15}H_{22}$	1-Methyldiamantane	1-MD
27	$C_{16}H_{24}$	1,4- + 2,4-Dimethyldiamantane	1,4- + 2,4-DMD
28	$C_{16}H_{24}$	4,8-Dimethyldiamantane	4,8-DMD
29	$C_{17}H_{26}$	1,4,9-Trimethyldiamantane	1,4,9-TMD
30	$C_{15}H_{22}$	3-Methyldiamantane	3-MD
31	$C_{16}H_{24}$	3,4-Dimethyldiamantane	3,4-DMD
32	$C_{17}H_{26}$	3,4,9-Trimethyldiamantane	3,4,9-TMD
I.S.-2	$C_{16}D_{34}$	*n*-Hexadecane-d_{34}	*n*-C_{16}-d_{34}

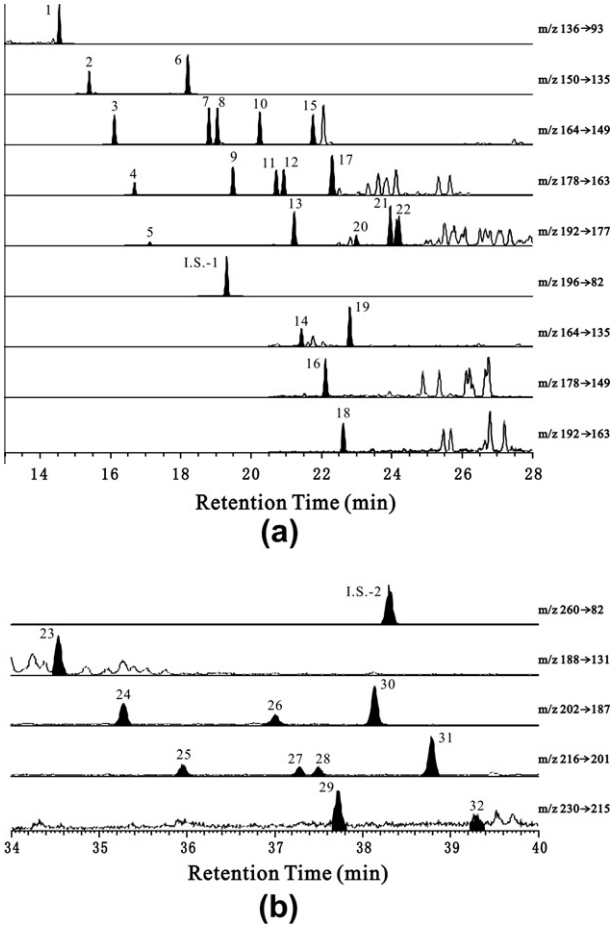

Fig. 2. GC–MS–MS chromatograms of diamondoids in the vessel obtained at 456 °C under the heating rate of 2 °C/h (EasyRo = 2.1%): (a) adamantanes, (b) diamantanes. Peak numbers are identified in Table 1.

Table 2
The yields (μg/g oil) of individual diamondoid compounds identified in Table 1 at each heating temperature of pyrolysis experiments.

Compound	Heating temperature (20 °C/h)										Heating temperature (2 °C/h)							
	336 °C	360 °C	382 °C	408 °C	432 °C	456 °C	480 °C	504 °C	528 °C	552 °C	336 °C	360 °C	384 °C	408 °C	432 °C	456 °C	480 °C	528 °C
A	nd	nd	nd	0.47	1.72	4.68	14.5	15.9	2.04	nd	nd	0.09	0.31	2.32	9.80	20.0	7.83	nd
1-MA	0.09	0.22	0.34	3.28	7.78	11.6	35.3	47.1	17.1	0.15	0.30	1.09	3.86	7.25	25.8	50.7	39.1	nd
1,3-DMA	0.15	0.15	0.19	0.61	1.96	6.74	20.9	33.7	24.3	0.94	0.27	0.37	0.59	3.71	15.3	31.7	41.2	nd
1,3,5-TMA	0.17	0.22	0.21	0.37	0.61	1.15	4.97	8.64	10.0	0.72	0.18	0.26	0.32	0.43	3.63	8.05	13.3	0.12
1,3,5,7-TeMA	nd	nd	nd	nd	nd	nd	0.68	1.06	0.31	0.78	nd	nd	nd	nd	0.45	0.93	1.70	0.14
2-MA	0.50	0.11	0.21	0.75	4.20	16.0	44.9	37.3	2.72	nd	0.17	0.33	1.85	8.69	35.8	57.1	12.2	nd
1,4-DMA(*cis*)	0.02	0.10	0.32	1.53	5.24	11.5	31.9	34.9	6.27	0.10	0.19	0.39	2.31	7.38	26.5	44.0	20.7	0.02
1,4-DMA(*trans*)	0.10	0.12	0.36	0.67	3.73	11.2	30.9	35.0	6.23	0.17	0.27	0.12	1.35	7.10	26.6	43.9	21.3	0.03
1,3,6-TMA	0.35	0.32	0.42	0.59	2.23	5.53	15.1	19.8	7.71	0.30	0.56	0.57	1.30	3.54	12.6	21.4	18.6	0.04
1,2-DMA	0.75	1.01	1.38	3.66	8.76	12.2	31.1	30.5	3.07	nd	1.12	2.21	7.82	10.0	28.7	41.0	13.6	nd
1,3,4-TMA(*cis*)	0.81	0.89	1.17	1.36	2.96	6.02	14.3	17.1	5.66	0.12	1.14	1.14	2.45	4.75	13.0	20.0	14.9	nd
1,3,4-TMA(*trans*)	1.03	1.14	1.35	2.13	5.52	7.12	14.2	17.1	5.78	0.08	1.25	1.51	3.87	6.40	14.1	19.3	14.4	nd
1,2,5,7-TeMA	0.86	0.94	1.06	0.95	1.68	2.87	7.49	11.3	7.03	0.29	1.12	1.09	1.81	2.70	6.94	11.1	12.7	0.14
1-EA	0.52	0.73	0.87	1.92	3.58	6.62	12.8	11.1	0.52	nd	0.94	1.03	2.77	5.26	11.8	15.6	3.79	nd
2,6- + 2,4-DMA	1.09	1.42	1.83	2.57	5.47	14.7	31.6	16.5	0.94	nd	1.59	1.93	3.09	9.69	30.5	36.8	2.08	nd
1-E-3-MA	1.05	1.25	1.72	6.18	12.1	6.19	14.2	14.8	2.94	nd	nd	nd	1.69	4.35	12.8	18.2	9.80	nd
1,2,3-TMA	2.33	3.00	3.29	4.20	7.78	15.0	30.3	24.2	1.33	0.05	3.37	3.85	6.13	11.5	31.1	40.0	7.88	nd
1-E-3,5-DMA	0.17	0.09	0.13	0.84	0.61	0.65	2.73	3.30	1.00	0.06	0.11	0.07	0.19	0.83	2.47	4.09	2.64	nd
2-EA	2.00	2.59	2.83	3.81	6.75	10.5	13.8	3.23	0.20	nd	2.76	3.16	3.93	9.35	17.3	11.6	0.49	nd
1,3,5,6-TeMA	0.59	0.86	0.16	0.16	1.08	0.58	1.54	1.73	0.28	nd	0.06	0.11	0.83	0.83	1.42	2.31	1.96	nd
1,2,3,5-TeMA	2.22	2.34	2.74	2.75	5.12	6.60	11.9	7.81	1.16	nd	2.68	2.96	4.18	5.65	12.2	13.8	2.59	nd
1-E-3,5,7-TMA	3.07	3.40	3.85	3.48	6.37	7.18	13.5	11.9	0.91	nd	4.01	4.30	5.63	7.89	13.3	17.3	5.69	nd
D	nd	nd	nd	nd	nd	5.69	8.26	10.7	9.29	1.04	nd	nd	nd	nd	7.90	12.2	15.0	0.20
4-MD	15.2	17.0	16.4	15.8	17.4	18.5	23.6	26.2	25.5	8.63	19.7	17.3	20.3	23.8	23.1	27.1	34.6	0.65
4,9-DMD	4.46	4.19	4.09	4.30	3.76	4.08	5.31	6.48	7.87	3.90	5.47	5.14	4.60	5.35	5.45	7.24	9.45	0.26
1-MD	nd	nd	nd	nd	nd	nd	nd	13.0	10.4	0.89	nd	nd	nd	nd	nd	13.4	16.1	0.26
1,4- + 2,4-DMD	1.51	2.19	2.39	2.33	1.41	2.04	3.29	5.11	5.88	0.73	2.85	4.25	2.03	1.35	2.82	5.59	8.28	0.42
4,8-DMD	6.53	7.64	8.29	7.39	7.88	3.33	3.58	4.80	4.85	0.67	10.2	11.0	9.33	11.6	3.72	5.43	7.33	0.27
1,4,9-TMD	1.29	1.37	1.37	1.21	1.36	0.97	1.19	1.85	2.29	0.61	1.53	1.67	1.69	1.38	1.68	1.71	2.70	0.55
3-MD	17.4	20.7	19.9	21.8	22.0	17.4	27.0	43.9	33.3	5.07	25.8	25.9	25.3	23.4	26.8	45.3	53.4	0.99
3,4-DMD	11.6	12.5	12.9	13.2	13.3	11.9	17.8	25.2	23.2	5.57	13.0	13.6	15.1	16.4	17.5	26.0	33.0	0.10
3,4,9-TMD	0.67	0.63	0.55	0.72	0.92	0.57	0.76	0.69	0.54	nd	0.92	0.59	0.70	0.66	0.57	0.72	1.02	nd

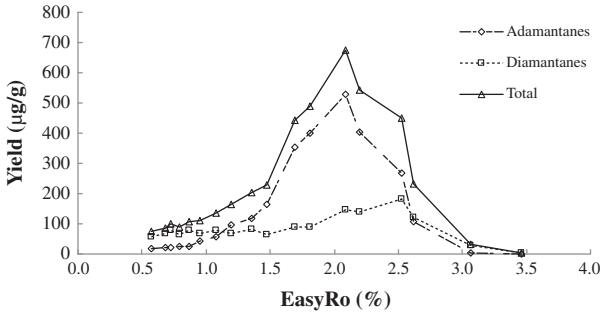

Fig. 3. Variation in the yields (μg/g oil) of diamondoids with EasyRo (%) in the oil-cracking experiment. (Total = sum of adamantanes and diamantanes displayed in Table 1.)

hydrocarbons gradually increases and reaches a maximum at 2.1% EasyRo. This result shows that oil cracking is dominated by C_6–C_{12} hydrocarbon cracking to C_2–C_5 hydrocarbons. At EasyRo > 2.1%, the cracking of C_2–C_5 hydrocarbons becomes the main source of methane, indicating the entrance of the oil cracking into the dry gas stage (corresponding to 2.1–4.5% EasyRo).

3.2. Abundance of diamondoids

Wei et al. (2007b) suggested that the concentration of diamondoids could be used as a maturity indicator for source rocks and oils. They established diamondoid–Ro equations from pyrolysis experiments on a few immature source rocks. However, the relations were constrained by few data (3–4 points) in their work (Wei et al., 2007b), which probably influences the accuracy of the equations.

In this study, 32 diamondoid compounds were identified by GC–MS–MS: 22 were adamantanes and 10 were diamantanes (Table 1 and Fig. 2). The yields of the individual diamondoid compounds at each temperature point were calculated based on the amount of diamondoids determined in the vessels and the initial weight of the oil in each gold tube (Table 2). Fig. 3 shows the changes in the yields of (a) total diamondoids, (b) adamantanes and (c) diamantanes with increased oil cracking. Total diamondoids refers to the sum of all 32 adamantanes and diamantanes listed in Table 1. For the oil at 336 °C at the heating rate of 20 °C/h (EasyRo < 0.6%), the yields of adamantanes and diamantanes were 17.9 and 58.7 μg/g, respectively. This implies that the formation of diamondoids might have begun in the oil window or even before. As shown in Fig. 3, the yield of diamondoids progressively increases from 76.5 μg/g to 673.6 μg/g within the EasyRo range of 1.0–2.1%, and then quickly decreases from the maximum at 2.1% EasyRo to 4.2 μg/g at 3.5% EasyRo. This indicates that diamondoids are mainly generated within the condensate and wet gas stages of oil cracking and are destroyed within the range of 2.1–3.5% EasyRo, corresponding to the dry gas stage. The diamondoids derived from the oil cracking are dominated by adamantanes (Fig. 3). The amount of generated diamantanes, ranging from 3.7–180.8 μg/g, is less than that of adamantanes, which vary from 0.5–528.9 μg/g and the generation curve occurs shows an obvious lag compared to adamantanes. For example, diamantanes are generated at ca. 1.7% EasyRo, reach a maximum yield at 2.5% EasyRo, and then quickly decompose.

The concentration of 3- + 4-methyldiamantanes was used to estimate the extent of oil cracking (Dahl et al., 1999). Fig. 4a shows that the yields of A (adamantane), MA (methyladamantanes), EA (ethyladamantanes), DMA (dimethyladamantanes) and TMA (trimethyladamantanes) increase with EasyRo in the range of 1.0–2.1%, and rapidly decrease in the EasyRo range 2.1–2.5%, suggesting that the parameters based on adamantanes are associated with the generation of diamondoids in the EasyRo range 1.0–2.1%. However, the parameters are influenced by the decomposition of diamondoids when EasyRo > 2.1%. Similarly, the yields of D (diamantane), MD (methyldiamantanes), and DMD (dimethyldiamantanes) increase in the EasyRo range 1.5–2.5% and a reversal occurs above the 2.5% EasyRo (Fig. 4b), suggesting that the diamantane parameters are useful in the range 1.5–2.5% EasyRo. In addition, Fig. 4 shows that adamantanes generated during oil cracking are dominated by dimethyladamantanes, followed by trimethyladamantanes, methyladamantanes, ethyladamantanes and adamantane, while diamantanes are dominated by methyldiamantanes, followed by dimethyldiamantanes and diamantane.

In summary, high concentrations of diamondoids in crude oil correspond to the maturity range from the wet gas (1.5–2.1% EasyRo) to the early dry gas (2.1–2.5% EasyRo) stages of oil cracking. In addition to the decomposition of the non-diamondoid compounds in crude oils, generation of diamondoids during oil cracking may also significantly contribute to their high concentrations.

3.3. Molecular composition of diamondoids

Fig. 5 shows the changes in the molecular composition of the diamondoids in the pyrolysates within the EasyRo range < 1.0–3.5%. First, only trace adamantanes and low yields of diamantanes are detected in the oil samples having EasyRo < 1.0% (Fig. 5a). Subsequently, the adamantane series begins to be generated when the EasyRo reaches 1.2% (Fig. 5b), and thereafter gradually increases (Fig. 5b–d). Diamantane series also increase within the range

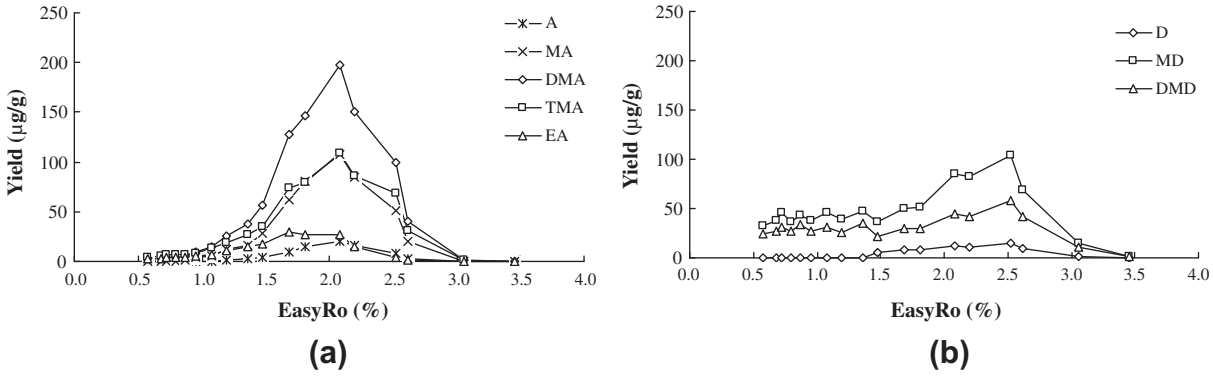

Fig. 4. Variation in the yields (μg/g oil) of different types of diamondoids with EasyRo (%) in the oil-cracking experiment: (a) adamantanes, (b) diamantanes. A = adamantane, MA = methyladamantanes, EA = ethyladamantanes, DMA = dimethyladamantanes, TMA = trimethyladamantanes, D = diamantane, MD = methyldiamantanes, DMD = dimethyldiamantanes.

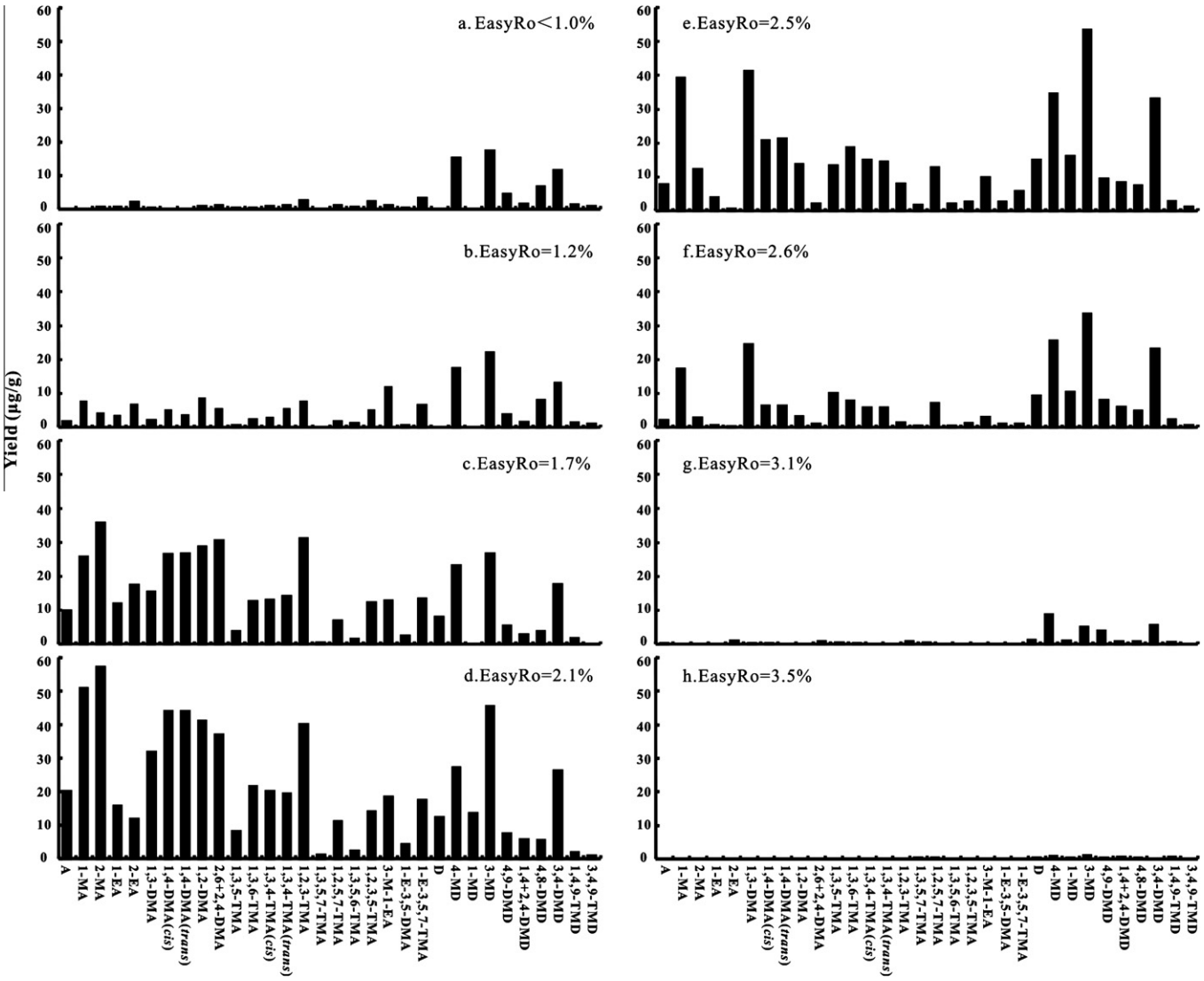

Fig. 5. Typical molecular composition of diamondoid hydrocarbons during oil cracking.

1.7–2.5% EasyRo (Fig. 5c–e). At higher maturity (EasyRo > 2.1%), adamantane compounds rapidly decrease and are completely destroyed at about 3.1% EasyRo (Fig. 5g). Similarly, the decomposition of diamantanes occurs at EasyRo > 2.5% (Fig. 5e–g), and they nearly disappear at EasyRo = 3.5% (Fig. 5h).

1-MA (compound 2 in Fig. 2), which has a methyl group attached to a bridgehead position, is more stable than 2-MA (compound 6 in Fig. 2) (Clark et al., 1979; Wingert, 1992). Similarly, 4-MD (compound 24 in Fig. 2) is more thermally stable than the other two isomers 1-MD and 3-MD (compounds 26 and 30 in Fig. 2, respectively) (Wingert, 1992; Chen et al., 1996). Hence, the ratios of MAI [methyl adamantane index, 1-MA/(1-MA + 2-MA)] and MDI [methyl diamantane index, 4-MD/(4-MD + 1-MD + 3-MD)] were introduced to evaluate highly mature crude oils or source rocks (Chen et al., 1996; Schulz et al., 2001; Wei et al., 2006b, 2007b). Some other ratios, such as MA/A [=(1-MA + 2-MA)/A], MDIA/DIA [=(1-MD + 3-MD + 4-MD)/D], EAI [=2-EA/(1-EA + 2-EA)], DMAI-1 [=1,3-DMA/(1,2-DMA + 1,3-DMA)], DMAI-2 [=1,3-DMA/(1,2-DMA + 1,4-DMA)], TMAI-1 [=1,3,5-TMA/(1,3,5-TMA + 1,3,4-TMA)], TMAI-2 [=1,3,5-TMA/(1,3,5-TMA + 1,3,6-TMA)], DMDI-1 [=3,4-DMD/(4,9-DMD + 3,4-DMD)] and DMDI-2 [=4,8-DMD/(4,9-DMD + 4,8-DMD)] have also been used (Grice et al., 2000; Schulz et al., 2001; Zhang et al., 2005; Wei et al., 2007b). Three ratios (DMDI-1, DMDI-2 and EAI) have been proposed to distinguish source facies (Schulz et al., 2001). Therefore, these parameters based on the relative concentrations of diamondoid isomers are used to characterize the variations in abundance and distribution of diamondoids during oil cracking in our study.

Previous studies suggested that the diamondoid maturity indices (e.g., MAI and MDI) only apply within a very narrow range. For example, MDI, varying from 40% to 65%, was only useful within the range of 0.9–2.0% Ro (Li et al., 2000). Schulz et al. (2001) suggested that the MAI and MDI only work for samples with maturities above 1.3% Ro, which is also supported by hydrous pyrolysis experiments (Wei et al., 2007a). The present quantitative data demonstrates that adamantanes from oil cracking were mainly produced within the maturity range 1.0–2.1% EasyRo, and were degraded at >2.1% EasyRo. In contrast, diamantanes were generated within the maturity range of 1.5–2.5% EasyRo, and destroyed at >2.5% EasyRo. Therefore, in addition to the differences among the thermal stabilities of isomers, the relative generation and decomposition rates of the isomers also influence their composition during thermal maturation. As shown in Fig. 6, there is no clear correlation in the plots of MAI and MDI versus EasyRo, showing that the two ratios are not useful to assess the maturity of oils.

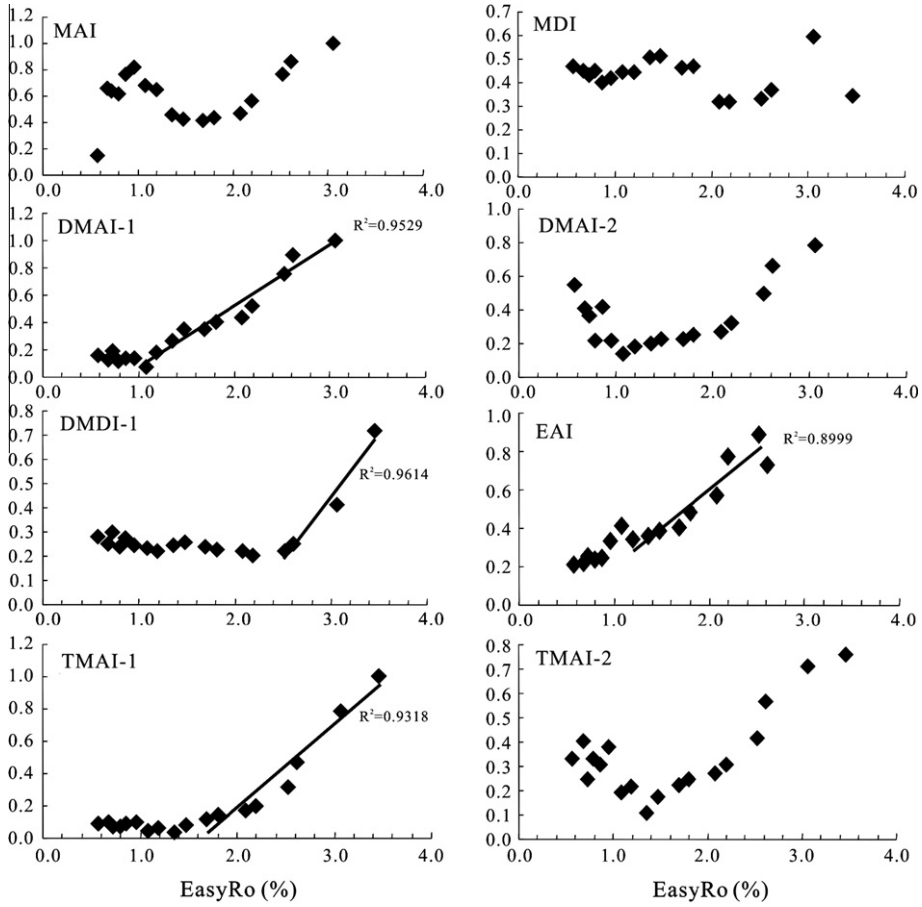

Fig. 6. Plots showing the variation of diamondoid indices (MAI, MDI, DMAI-1, DMAI-2, DMDI-1, EAI, TMAI-1 and TMAI-2) with EasyRo (%). MAI = 1-MA/(1-MA + 2-MA), MDI = 4-MD/(4-MD + 1-MD + 3-MD), DMAI-1 = 1,3-DMA/(1,2-DMA + 1,3-DMA), DMAI-2 = 1,3-DMA/(1,2-DMA + 1,4-DMA), DMDI-1 = 3,4-DMD/(4,9-DMD + 3,4-DMD), EAI = 2-EA/(1-EA + 2-EA), TMAI-1 = 1,3,5-TMA/(1,3,5-TMA + 1,3,4-TMA), TMAI-2 = 1,3,5-TMA/(1,3,5-TMA + 1,3,6-TMA).

Good linear relationships are displayed between EasyRo and a few diamondoid parameters, such as DMAI-1 in the range 1.0–3.0% EasyRo, TMAI-1 in the range 1.5–3.5% EasyRo, EAI in the range 1.0–2.5% EasyRo, and DMDI-1 in the range 2.5–3.5% EasyRo (Fig. 6). DMAI-2 and TMAI-2 also increase with EasyRo above 1.0% and 1.5%, respectively. However, below the EasyRo of 1.0% for DMAI-2 or 1.5% for TMAI-2, a reverse trend is observed (Fig. 6), which is probably due to mixing of new components generated from oil cracking and the early formed residue in the oils. These ratios cover a relatively wide maturity range from 1.0% to 3.5% EasyRo, especially DMAI-1 and TMAI-1, whose useful ranges include 1.0–3.0% and 1.5–3.5%, respectively. Therefore, the four parameters with both linearity and monotonicity, DMAI-1, DMDI-1, TMAI-1 and EAI, are probably good indicators of thermal maturity.

4. Conclusions

A simulation experiment of oil cracking combined with quantification of diamondoids in the vessels was carried out. The results indicate that diamondoids are mainly generated during the condensate and wet gas stages of oil cracking (1.0–2.1% EasyRo) and destroyed at EasyRo > 2.1%. High concentrations of diamondoids in crude oils correspond to the maturity range from the wet gas (1.5–2.1% EasyRo) to the early dry gas (2.1–2.5% EasyRo) stages of oil cracking. MAI and MDI are commonly used maturity indices, but their use to evaluate oil maturity is not supported by the present experimental results. In contrast, some other diamondoid parameters, such as EAI, DMAI-1, DMDI-1 and TMAI-1 correlate with thermal maturity expressed by EasyRo (%), indicating that they can be useful indicators to assess the thermal maturity of oils.

Acknowledgements

This work was financially supported by the National Natural Science Foundation of China (Grant No. 41172115), and National Science & Technology Major Project of the Ministry of Science and Technology of China (Grant No. 2011ZX05008-002-32). This is Contribution No. IS-1425 from GIGCAS. We are grateful to Dr. Zhang W.B. for his assistance with GC–MS–MS analysis and Dr. Zhang H.Z. for the provision of the Tarim Basin oil sample. We also thank K.E. Peters and an anonymous reviewer for their constructive comments and suggestions.

Associate Editor—**Ken Peters**

References

Berwick, L., Alexander, R., Pierce, K., 2011. Formation and reactions of alkyl adamantanes in sediments: carbon surface reactions. Organic Geochemistry 42, 752–761.

Chen, J.H., Fu, J.M., Sheng, G.Y., Liu, D.H., Zhang, J.J., 1996. Diamondoid hydrocarbon ratios: novel maturity indices for highly mature crude oils. Organic Geochemistry 25, 179–190.

Clark, T., Knox, T.M.O., McKervey, M.A., Mackle, H., Rooney, J.J., 1979. Thermochemistry of bridged-ring substances – enthalpies of formation of some diamondoid hydrocarbons and of perhydroquinacene – comparisons with data from empirical force-field calculations. Journal of the American Chemical Society 101, 2404–2410.

Dahl, J.E., Moldowan, J.M., Peters, K.E., Claypool, G.E., Rooney, M.A., Michael, G.E., Mello, M.R., Kohnen, M.L., 1999. Diamondoid hydrocarbons as indicators of natural oil cracking. Nature 399, 54–57.

Fang, C.C., Xiong, Y.Q., Liang, Q.Y., Li, Y., Peng, P.A., 2011. Optimization of headspace single-drop microextraction technique for extration of light hydrocarbons (C_6–C_{12}) and its potential applications. Organic Geochemistry 42, 316–322.

Fort, R.C., Schleyer, P.V., 1964. Adamantane – consequences of diamondoid structure. Chemical Reviews 64, 277–300.

Giruts, M.V., Gordadze, G.N., 2007. Generation of adamantanes and diamantanes by thermal cracking of polar components of crude oils of different genotypes. Petroleum Chemistry 47, 12–22.

Giruts, M.V., Rusinova, G.V., Gordadze, G.N., 2006. Generation of adamantanes and diamantanes by thermal cracking of high-molecular-mass saturated fractions of crude oils of different genotypes. Petroleum Chemistry 46, 225–236.

Gordadze, G.N., Giruts, M.V., 2008. Synthesis of adamantane and diamantane hydrocarbons by high-temperature cracking of higher *n*-alkanes. Petroleum Chemistry 48, 414–419.

Grice, K., Alexander, R., Kagi, R.I., 2000. Diamondoid hydrocarbon ratios as indicators of biodegradation in Australian crude oils. Organic Geochemistry 31, 67–73.

Hill, R.J., Tang, Y.C., Kaplan, I.R., 2003. Insights into oil cracking based on laboratory experiments. Organic Geochemistry 34, 1651–1672.

Li, J.G., Philp, P., Cui, M.Z., 2000. Methyl diamantane index (MDI) as a maturity parameter for Lower Palaeozoic carbonate rocks at high maturity and overmaturity. Organic Geochemistry 31, 267–272.

Li, S.M., Pang, X.Q., Jin, Z.J., Yang, H.J., Xiao, Z.Y., Gu, Q.Y., Zhang, B.S., 2010. Petroleum source in the Tazhong Uplift, Tarim Basin: new insights from geochemical and fluid inclusion data. Organic Geochemistry 41, 531–553.

Liang, Q.Y., Xiong, Y.Q., Fang, C.C., Li, Y., 2012. Quantitative analysis of diamondoids in crude oils using gas chromatography – triple quadrupole mass spectrometry. Organic Geochemistry 43, 83–91.

Oya, A., Nakamura, H., Otani, S., Marsh, H., 1981. Carbonization of adamantane to a graphitizable carbon. Fuel 60, 667–669.

Petrov, A., Arefjev, D.A., Yakubson, Z.V., 1974. Hydrocarbons of adamantane series as indices of petroleum catagenesis. In: Tissot, B., Bienner, F. (Eds.), Advances in organic geochemistry. Editions Technip, Paris, pp. 517–522.

Schneider, A., Warren, R.W., Janoski, E.J., 1966. Formation of perhydrophenalenes and polyalkyladamantanes by isomerization of tricyclic perhydroaromatics. Journal of Organic Chemistry 31, 1617–1625.

Schoell, M., Carlson, R.M.K., 1999. Diamondoids and oil are not forever. Nature 399, 15–16.

Schulz, L.K., Wilhelms, A., Rein, E., Steen, A.S., 2001. Application of diamondoids to distinguish source rock facies. Organic Geochemistry 32, 365–375.

Sweeney, J.J., Burnham, A.K., 1990. Evaluation of a simple model of vitrinite reflectance based on chemical-kinetics. American Association of Petroleum Geologists Bulletin 74, 1559–1570.

Wei, Z.B., Moldowan, J.M., Dahl, J., Goldstein, T.P., Jarvie, D.M., 2006a. The catalytic effects of minerals on the formation of diamondoids from kerogen macromolecules. Organic Geochemistry 37, 1421–1436.

Wei, Z., Moldowan, J.M., Jarvie, D.M., Hill, R., 2006b. The fate of diamondoids in coals and sedimentary rocks. Geology 34, 1013–1016.

Wei, Z.B., Moldowan, J.M., Paytan, A., 2006c. Diamondoids and molecular biomarkers generated from modern sediments in the absence and presence of minerals during hydrous pyrolysis. Organic Geochemistry 37, 891–911.

Wei, Z.B., Moldowan, J.M., Peters, K.E., Wang, Y., Xiang, W., 2007a. The abundance and distribution of diamondoids in biodegraded oils from the San Joaquin Valley: implications for biodegradation of diamondoids in petroleum reservoirs. Organic Geochemistry 38, 1910–1926.

Wei, Z.B., Moldowan, J.M., Zhang, S.C., Hill, R., Jarvie, D.M., Wang, H.T., Song, F.Q., Fago, F., 2007b. Diamondoid hydrocarbons as a molecular proxy for thermal maturity and oil cracking: geochemical models from hydrous pyrolysis. Organic Geochemistry 38, 227–249.

Wingert, W.S., 1992. GC–MS analysis of diamondoid hydrocarbons in Smackover petroleums. Fuel 71, 37–43.

Xiong, Y.Q., Geng, A.S., Liu, J.Z., 2004. Kinetic-simulating experiment combined with GC–IRMS analysis: application to identification and assessment of coal-derived methane from Zhongba gas field (Sichuan Basin, China). Chemical Geology 213, 325–338.

Zhang, S.C., Huang, H.P., Xiao, Z.Y., Liang, D.G., 2005. Geochemistry of Palaeozoic marine petroleum from the Tarim Basin, NW China: Part 2. Maturity assessment. Organic Geochemistry 36, 1215–1225.